Supplementary Data

Crystal chemistry of schreibersite, $(Fe,Ni)_3P$

Sergey N. Britvin, Maria G. Krzhizhanovskaya, Andrey A. Zolotarev, Liudmila A. Gorelova, Edita V. Obolonskaya, Natalia S. Vlasenko, Vladimir V. Shilovskih and Mikhail N. Murashko

Table S1. Chemical composition of schreibersite (wt.%)

Sample	Code	Fe	Co	Ni	P	Total
Hatrurim	Htr	83.45	0.17	0.91	15.75	100.28
Zacatecas (1792)	Zct	73.03	0.21	11.67	15.31	100.22
São Julião de Moreira	SJM	69.92	0.15	14.80	15.33	100.20
Madoc	Mad	66.68	0.16	17.07	15.61	99.52
Bischtübe	Bst	66.70	0.26	16.93	15.54	99.43
Toluca	Tol	66.42	0.22	18.07	15.32	100.03
Glorieta Mountain	GM	65.88	0.31	18.70	15.47	100.36
Augustinovka	Aug	63.21	0.21	20.92	15.34	99.68
Mont Dieu	MD	57.11	0.14	26.81	15.54	99.60
Lazarev	Lzr	55.81	0.31	28.86	15.06	100.04
Krasnojarsk	Krs	55.01	0.40	29.15	15.46	100.02
Seymchan	Sey	55.27	0.13	29.31	15.62	100.33
Brenham	Brh	54.72	0.19	29.31	15.36	99.58
Cranbourne	Crn1	54.08	0.23	29.98	15.58	99.87
Magura	Mgr	53.38	0.20	31.51	15.38	100.47
Canyon Diablo	CD1	51.92	0.12	32.71	15.22	99.97
Cosby's Creek	Csb	51.45	0.34	32.84	15.31	99.94
Petropavlovsk	Ptr	51.63	0.20	32.68	15.12	99.63
Springwater	Spr	51.21	0.37	33.37	15.41	100.36
Finmarken	Fnm2	47.99	0.45	36.41	15.26	100.11
Canyon Diablo	CD2	47.52	0.16	37.31	15.24	100.23
Finmarken	Fnm3	41.67	0.09	42.77	15.09	99.62
Cranbourne	Crn2	39.99	0.19	44.25	15.02	99.45

Table S2. Formula amounts of elements in schreibersite (*apfu*, calculated on 4 *apfu*)

Sample	**Code**	**Fe**	**Co**	**Ni**	**Σ*M***	**P**
Hatrurim	Htr	2.96	0.006	0.03	2.99	1.01
Zacatecas	Zct	2.61	0.007	0.40	3.01	0.99
São Julião de Moreira	SJM	2.50	0.005	0.50	3.01	0.99
Madoc	Mad	2.40	0.005	0.58	2.99	1.01
Bischtübe	Bst	2.40	0.009	0.58	2.99	1.01
Toluca	Tol	2.38	0.007	0.62	3.01	0.99
Glorieta Mountain	GM	2.36	0.011	0.64	3.01	1.00
Augustinovka	Aug	2.28	0.007	0.72	3.01	1.00
Mont Dieu	MD	2.06	0.005	0.92	2.99	1.01
Lazarev	Lzr	2.02	0.011	0.99	3.02	0.98
Krasnojarsk	Krs	1.98	0.014	1.00	2.99	1.00
Seymchan	Sey	1.98	0.004	1.00	2.98	1.01
Brenham	Brh	1.98	0.006	1.01	3.00	1.00
Cranbourne	Crn1	1.95	0.008	1.03	2.99	1.01
Magura	Mgr	1.92	0.007	1.08	3.01	1.00
Canyon Diablo	CD1	1.88	0.004	1.13	3.01	0.99
Cosby's Creek	Csb	1.86	0.012	1.13	3.00	1.00
Petropavlovsk	Ptr	1.87	0.007	1.13	3.01	0.99
Springwater	Spr	1.84	0.013	1.14	2.99	1.00
Finmarken	Fnm2	1.74	0.015	1.25	3.01	1.00
Canyon Diablo	CD2	1.72	0.005	1.28	3.01	0.99
Finmarken	Fnm3	1.52	0.003	1.48	3.00	0.99
Cranbourne	Crn2	1.46	0.007	1.54	3.01	0.99

Table S3. Summary of single-crystal data collection and refinement details for schreibersite

Code	I/σ	R_{int} (%)	Total reflections	Unique observed reflections	R_1 (%)	S
Htr	49.8	3.14	4137	615	1.56	1.054
Zct	64.0	2.06	3484	627	0.75	1.164
SJM	72.8	3.00	6193	637	0.96	1.280
Mad	76.4	2.19	5325	630	0.89	1.157
Bst	72.7	2.98	6317	639	0.96	1.288
Tol	66.8	3.24	6033	632	0.78	1.196
GM	45.8	3.44	4198	632	1.17	1.222
Aug	90.8	2.17	5319	632	0.75	1.118
MD	65.7	3.11	5108	634	1.07	1.264
Lzr	42.6	3.37	2989	636	1.11	1.127
Krs	47.8	3.42	4572	632	1.17	1.173
Sey	44.2	3.12	3772	623	1.12	1.008
Brh	55.4	2.99	4881	635	1.09	1.176
Crn1	66.7	2.16	4013	635	0.83	1.103
Mgr	36.0	3.79	3160	599	2.01	1.109
CD1	90.4	2.79	9470	630	0.78	1.203
Csb	30.6	5.44	3491	626	1.57	1.105
Ptr	32.9	3.68	2412	610	1.51	1.006
Spr	38.3	4.61	5282	618	1.47	1.136
Fnm2	34.3	4.28	2860	626	1.18	1.056
CD2	68.5	3.70	8193	629	0.80	1.174
Fnm3	61.8	3.66	5959	621	1.28	1.145
Crn2	42.7	318	3198	621	1.17	1.061

Table S4. Summary of the last loop Rietveld refinement results for schreibersite [a]

Code	R_p	R_{wp}	R_{exp}	*GoF*	R_B	*a* (Å)	*c* (Å)	*V* (Å^3)	*c*/*a*
Htr	0.36	0.58	0.41	1.43	0.33	9.1094	4.4624	370.30	0.4899
Zct	0.33	0.55	0.48	1.15	0.22	9.0856	4.4662	368.68	0.4916
SJM	0.90	1.46	0.45	3.27	0.78	9.0772	4.4650	367.90	0.4919
Mad	0.35	0.66	0.42	1.59	0.59	9.0748	4.4654	367.73	0.4921
Bst	0.79	1.54	0.43	3.55	1.19	9.0732	4.4650	367.57	0.4921
Tol	0.73	1.42	0.43	3.27	1.27	9.0720	4.4651	367.48	0.4922
GM	0.64	1.30	0.45	2.87	1.36	9.0700	4.4648	367.30	0.4923
Aug	0.21	0.33	0.45	0.74	0.35	9.0686	4.4661	367.29	0.4925
MD	0.51	1.00	0.42	2.39	0.78	9.0571	4.4660	366.35	0.4931
Lzr	0.28	0.48	0.42	1.14	0.30	9.0532	4.4656	366.00	0.4933
Krs	0.49	0.97	0.43	2.24	0.87	9.0494	4.4649	365.64	0.4934
Sey	0.20	0.33	0.45	0.73	0.24	9.0514	4.4647	365.78	0.4933
Brh	0.25	0.46	0.41	1.11	0.25	9.0497	4.4642	365.60	0.4933
Crn1	0.44	0.87	0.44	1.96	0.79	9.0471	4.4647	365.44	0.4935
Mgr	0.58	1.01	0.38	2.67	0.44	9.0473	4.4645	365.44	0.4935
CD1	0.77	1.44	0.42	3.40	0.93	9.0409	4.4638	364.86	0.4937
Csb	0.39	0.72	0.41	1.75	0.58	9.0435	4.4648	365.15	0.4937
Ptr	0.24	0.39	0.45	0.87	0.35	9.0449	4.4654	365.32	0.4937
Spr	0.46	0.95	0.42	2.27	1.24	9.0434	4.4645	365.12	0.4937
Fnm2	0.28	0.54	0.46	1.16	0.51	9.0413	4.4644	364.94	0.4938
CD2	0.66	1.23	0.40	3.04	0.94	9.0363	4.4644	364.54	0.4941
Fnm3	0.21	0.36	0.46	0.79	0.58	9.0282	4.4637	363.83	0.4944
Crn2	0.28	0.49	0.46	1.06	0.27	9.0249	4.4622	363.44	0.4944

[a] The 3rd refinement loop as described in the Materials and Methods section. Estimated standard deviations: *a* 5×10^{-4} Å; *c* 3×10^{-4} Å; *V* 0.05 Å^3. The unit-cell parameters, atomic coordinates, site occupancies and isotropic displacement parameters were freely refined, except for the Htr sample (Fe_3P end-member). Further details of the Rietveld refinements, experimental, calculated and background profiles can be retrieved from the powder CIF files attached to the Supplementary materials.

Table S5. Atomic scattering factors of Fe and Ni for Co*K*α and Mo*K*α radiation (sinΘ/λ = 0)

Radiation	**Element**	$Z = f_0$	f'	f''	$\lvert f \rvert$ [a]	**Difference (%)** [b]
Mo*K*α	Fe	26	0.3463	0.8444	26.36	7.30
(λ = 0.71073 Å)	Ni	28	0.3393	1.1124	28.36	
Co*K*α	Fe	26	–3.339	0.505	22.67	15.41
(λ = 1.79021 Å)	Ni	28	–1.555	0.691	26.46	

[a] $|f| = f_0 + \Delta f' - \frac{1}{2}\Delta f''/(f_0 + \Delta f')$ (e.g., Matthews, 2006)

[b] Difference (%) = $100 \times \frac{1}{2}[|f|(\text{Ni}) - |f|(\text{Fe})] / [|f|(\text{Ni}) + |f|(\text{Fe})]$

Matthews, B.W. (2006) Heavy atom location and phase determination with single wavelength diffraction data. International Tables for Crystallography; IUCr, Kluwer Academic Publishing, Dordrecht, The Netherlands, Vol. F, 293–298.

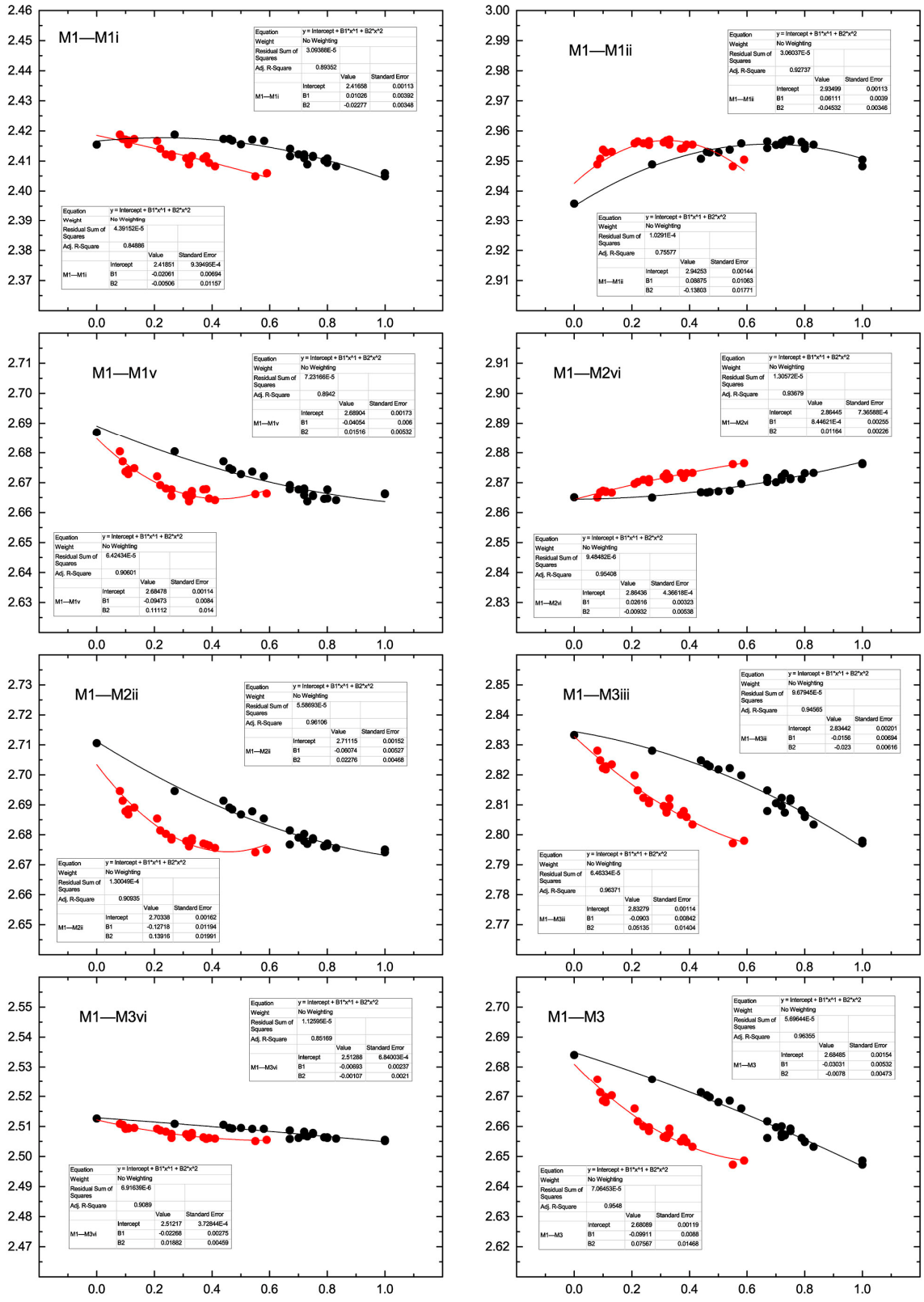

Figure S1. Site-specific dependencies of interatomic bond lengths on Ni site populations in schreibersite. Horizontal scale: Ni site population (*apfu*). Vertical scale: bond length (Å). Red circles, *M*2 site; black circles, *M*3 site. Symmetry codes: (i) –x, –y, z; (ii) y, –x, –z+1; (iii) –y, x, –z+1; (v) –y, x, –z; (vi) x, y, z–1.

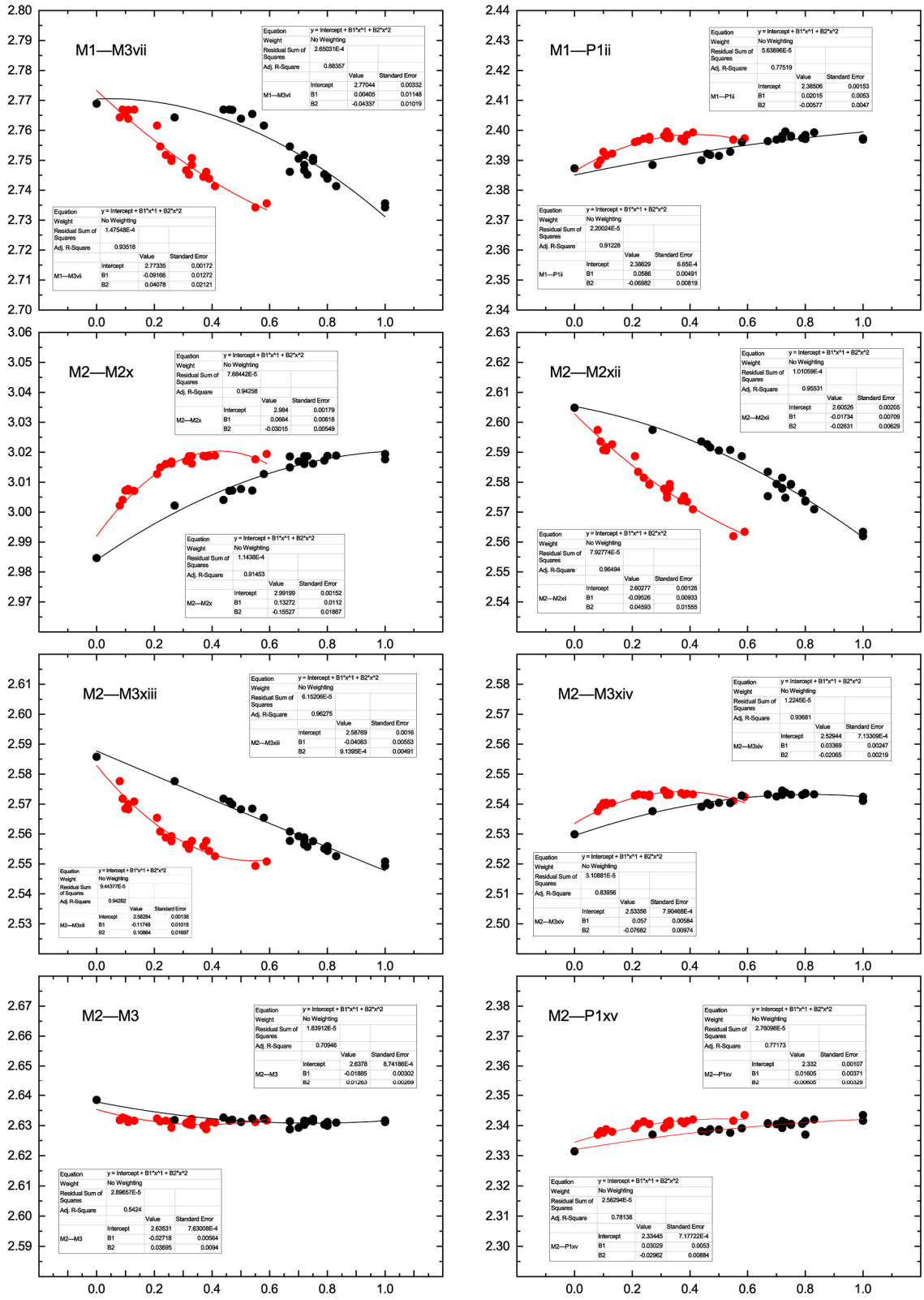

Figure S2. Site-specific dependencies of interatomic bond lengths on Ni site populations in schreibersite. Horizontal scale: Ni site population (*apfu*). Vertical scale: bond length (Å). Red circles, *M*2 site; black circles, *M*3 site. Symmetry codes: (ii) y, –x, –z+1; (vii) –x+1/2, –y–1/2, z–1/2; (viii) –y+1/2, x–1/2, –z+3/2; (ix) y+1/2, –x+1/2, –z+3/2; (x) y+1/2, –x+1/2, –z+5/2; (xii) –x+1, –y, z; (xv) x, y, z+1.

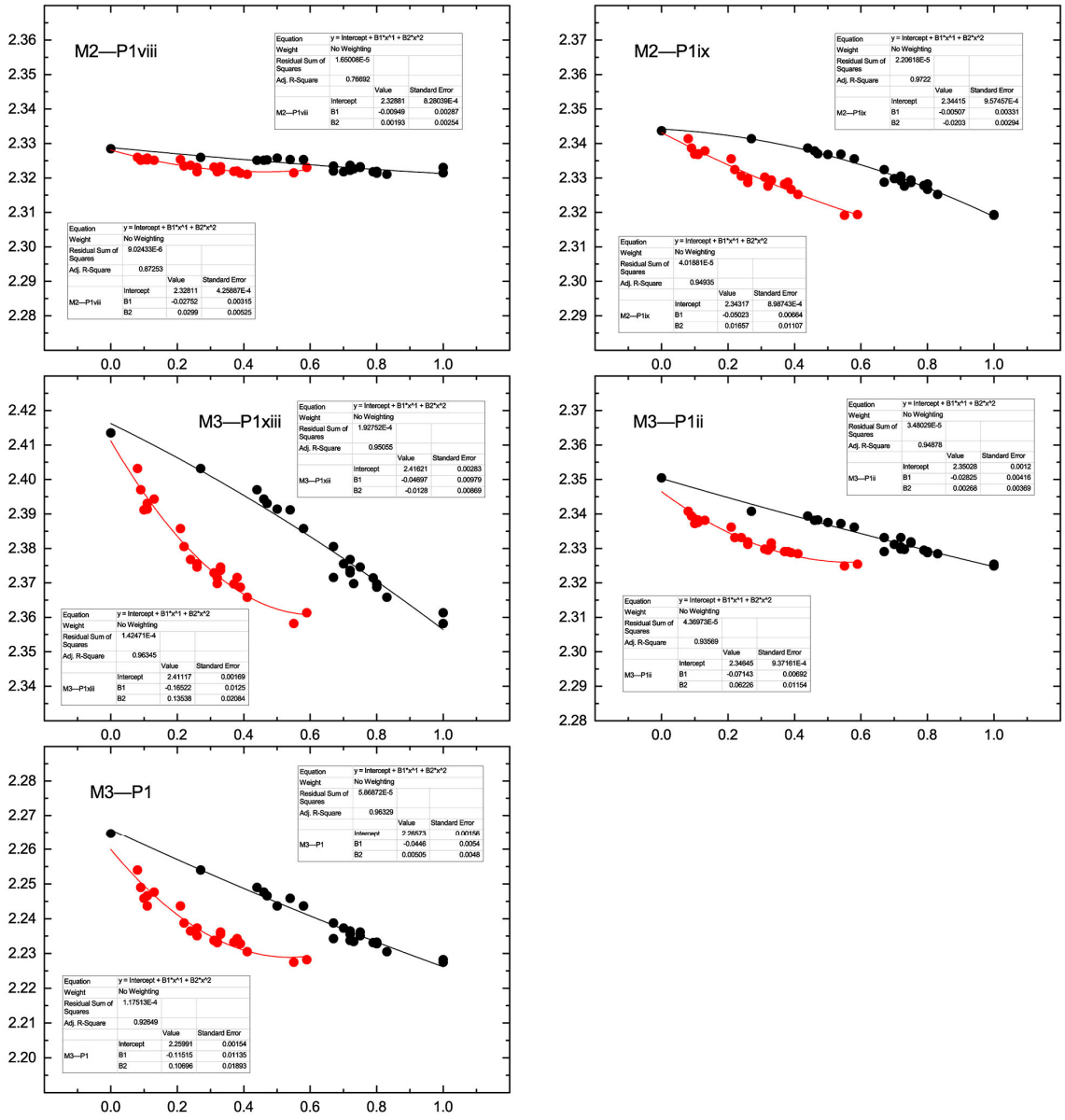

Figure S3. Site-specific dependencies of interatomic bond lengths on Ni site populations in schreibersite. Horizontal scale: Ni site population (*apfu*). Vertical scale: bond length (Å). Red circles, *M*2 site; black circles, *M*3 site. Symmetry codes: (ii) y, –x, –z+1; (viii) –y+1/2, x–1/2, –z+3/2; (ix) y+1/2, –x+1/2, –z+3/2.

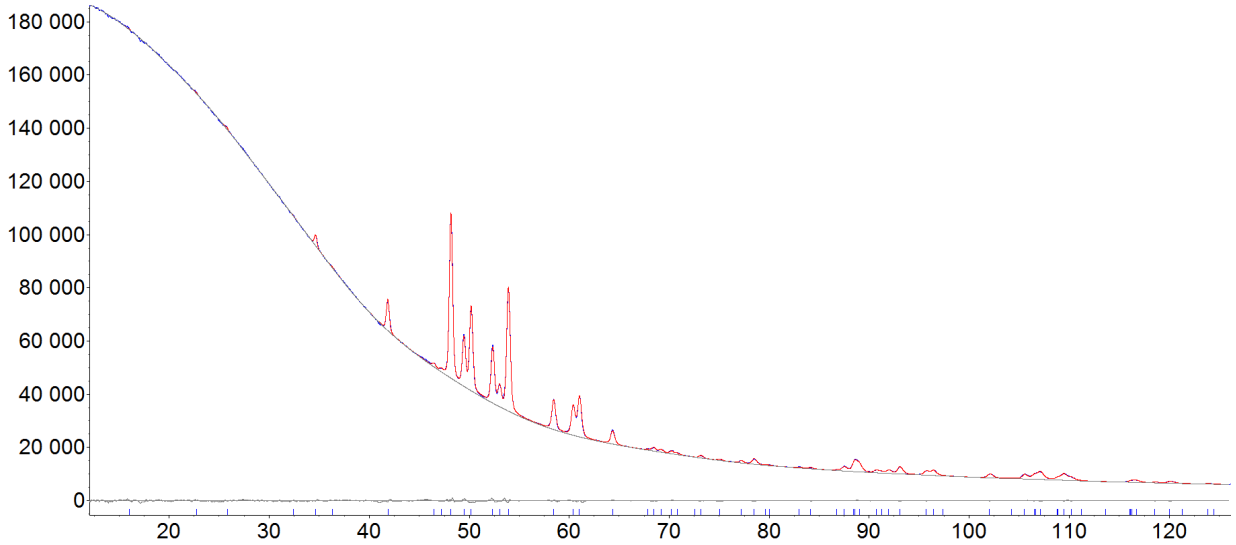

Figure S4. Rietveld refinement plot for schreibersite from the Augustinovka meteorite (Aug).

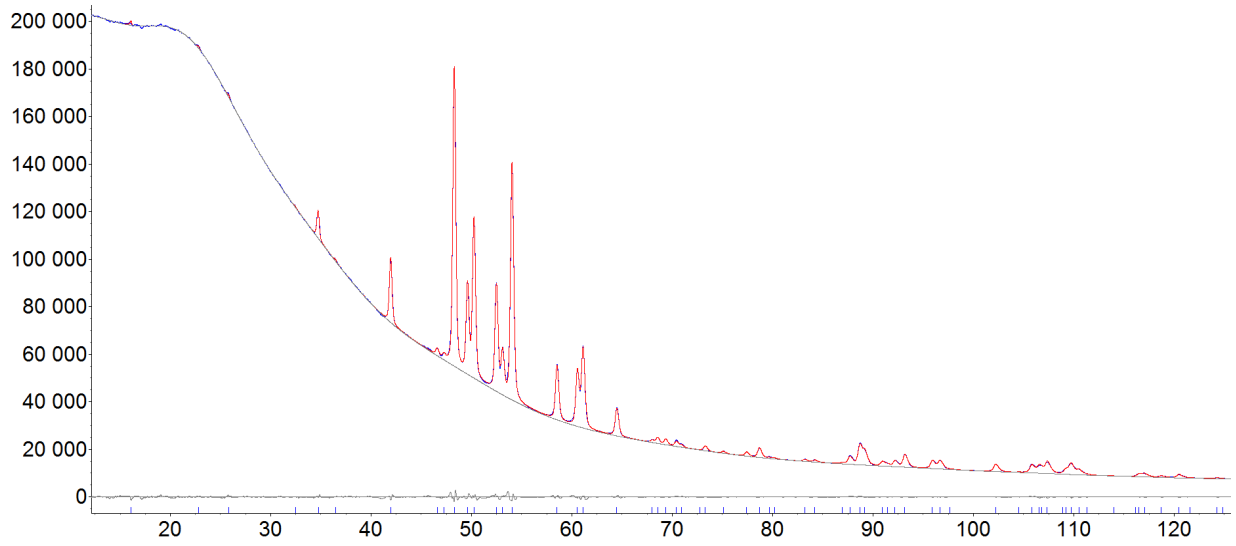

Figure S5. Rietveld refinement plot for schreibersite from the Brenham meteorite (Brh).

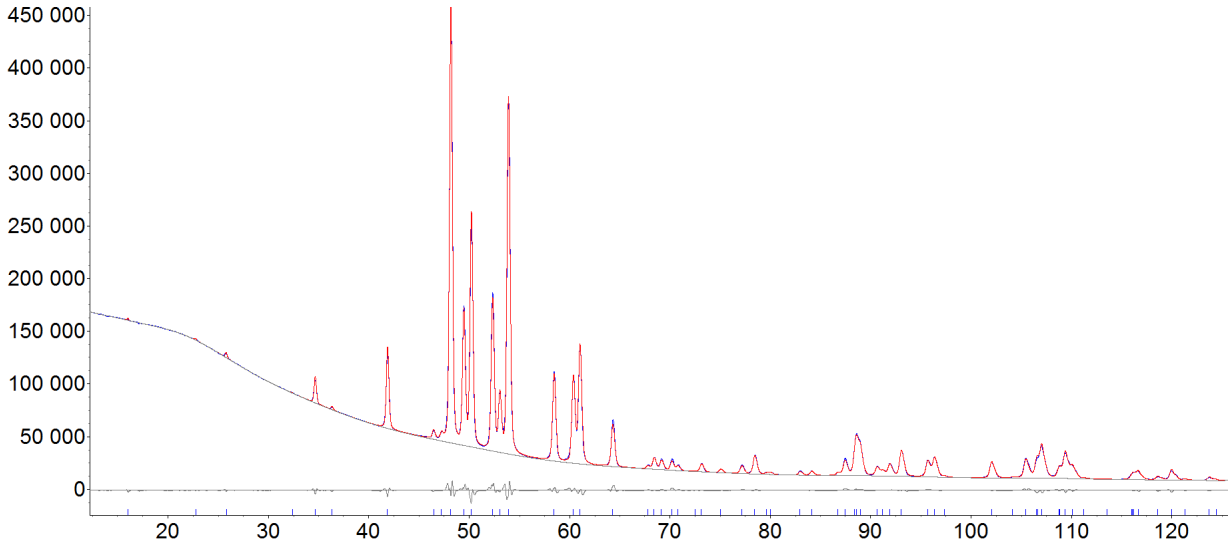

Figure S6. Rietveld refinement plot for schreibersite from the Bischtübe meteorite (Bst).

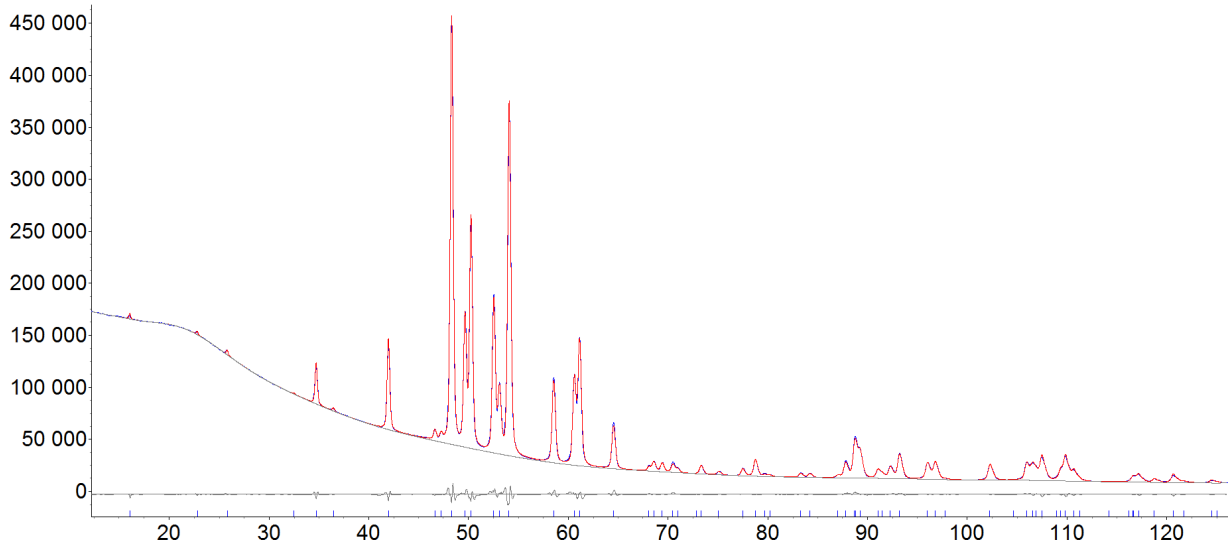

Figure S7. Rietveld refinement plot for schreibersite from the Canyon Diablo meteorite (CD1).

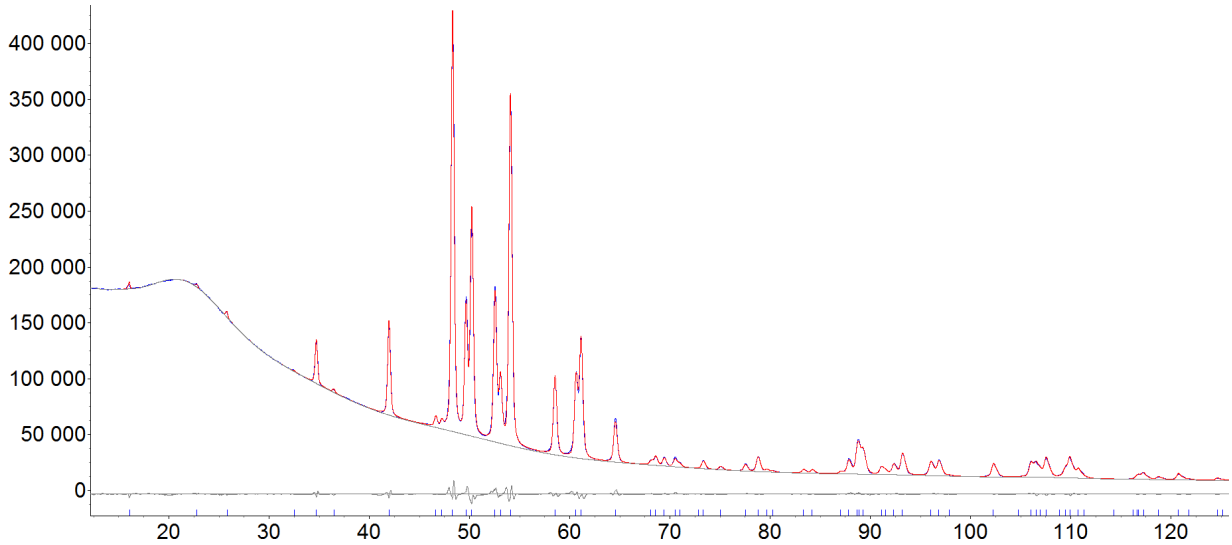

Figure S8. Rietveld refinement plot for schreibersite from the Canyon Diablo meteorite (CD2).

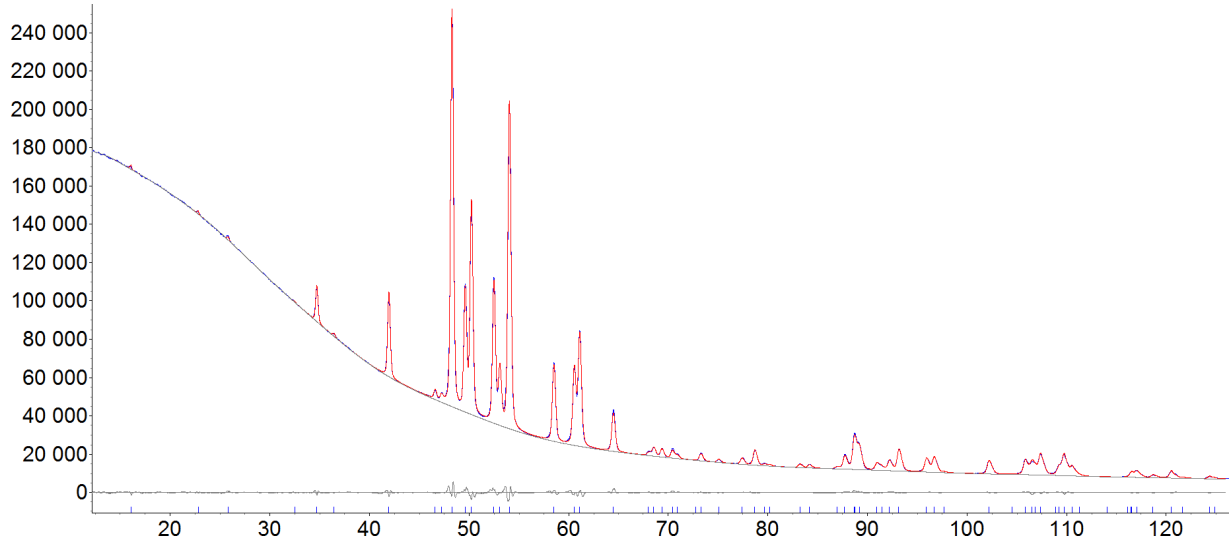

Figure S9. Rietveld refinement plot for schreibersite from the Cranbourne meteorite (Crn1).

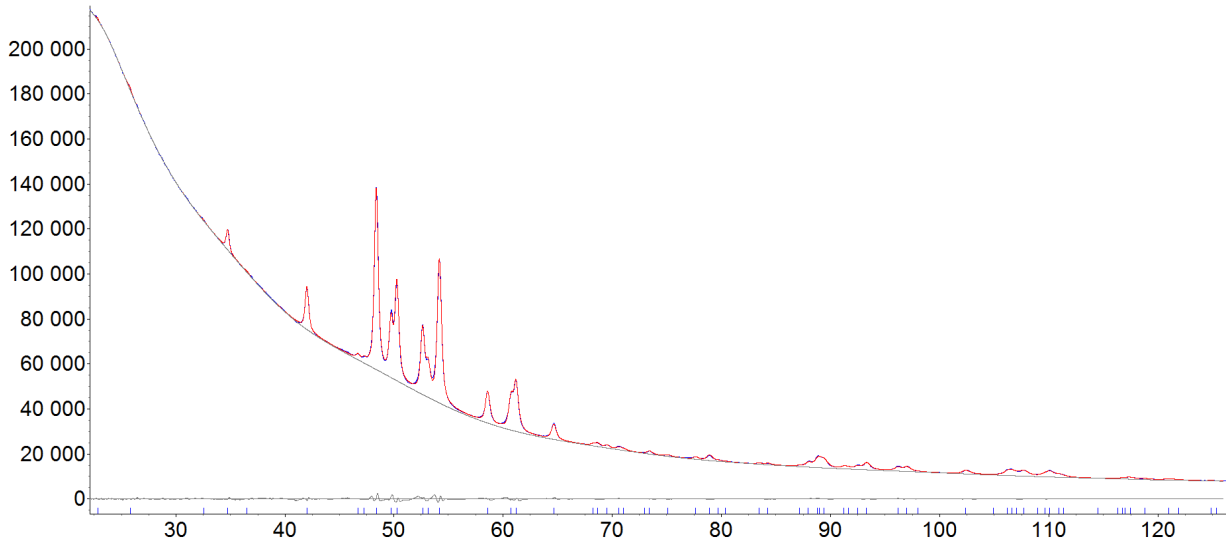

Figure S10. Rietveld refinement plot for nickelphosphide from the Cranbourne meteorite (Crn2).

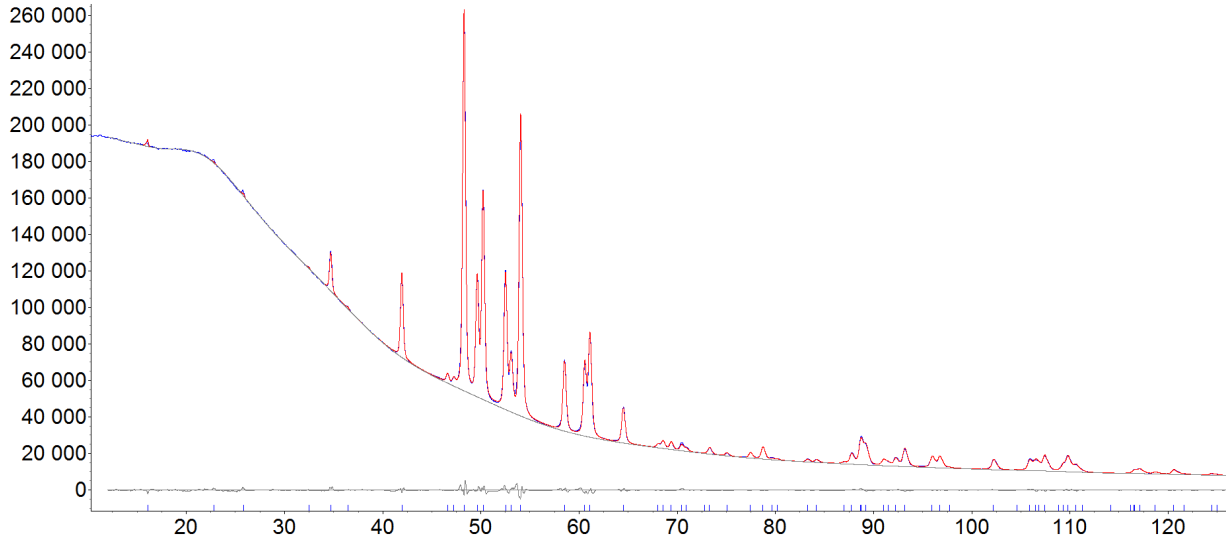

Figure S11. Rietveld refinement plot for schreibersite from the Cosby's Creek meteorite (Csb).

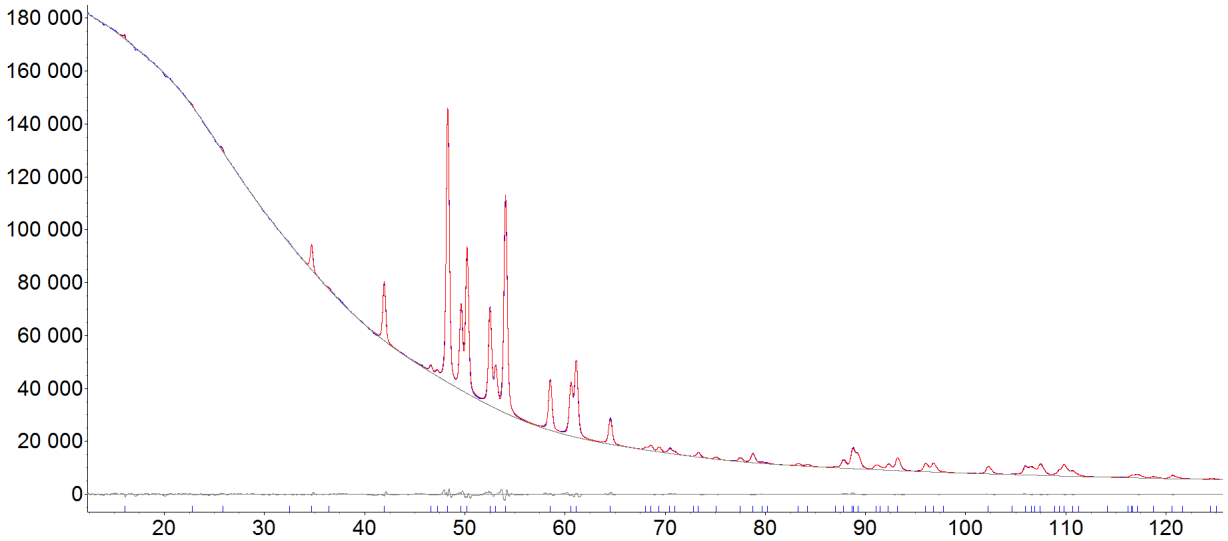

Figure S12. Rietveld refinement plot for schreibersite from the Finmarken meteorite (Fnm2).

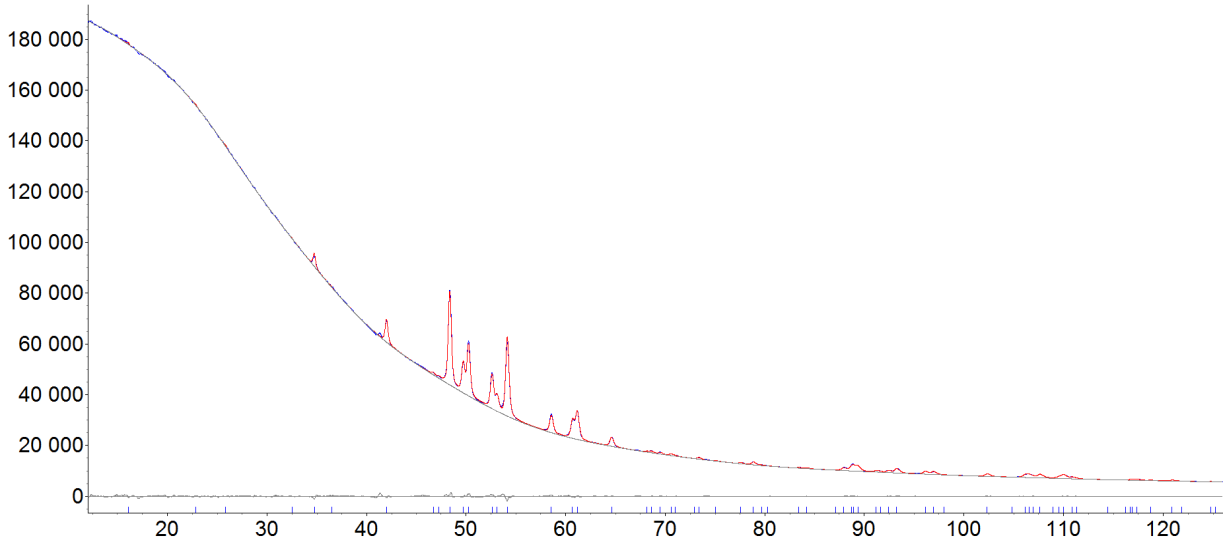

Figure S13. Rietveld refinement plot for nickelphosphide from the Finmarken meteorite (Fnm3).

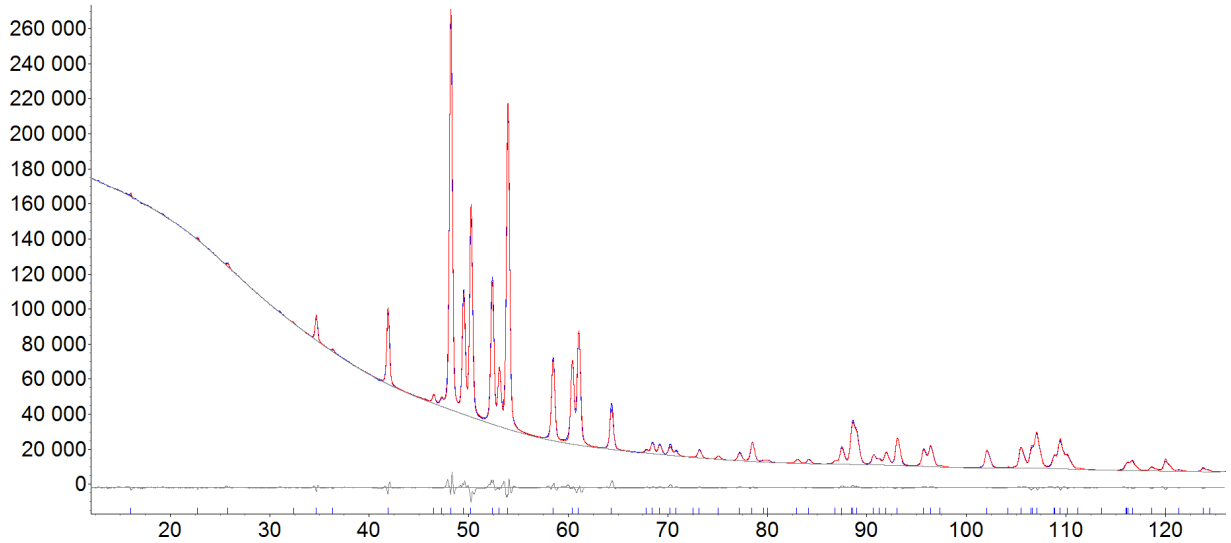

Figure S14. Rietveld refinement plot for schreibersite from the Glorieta Mountain meteorite (GM).

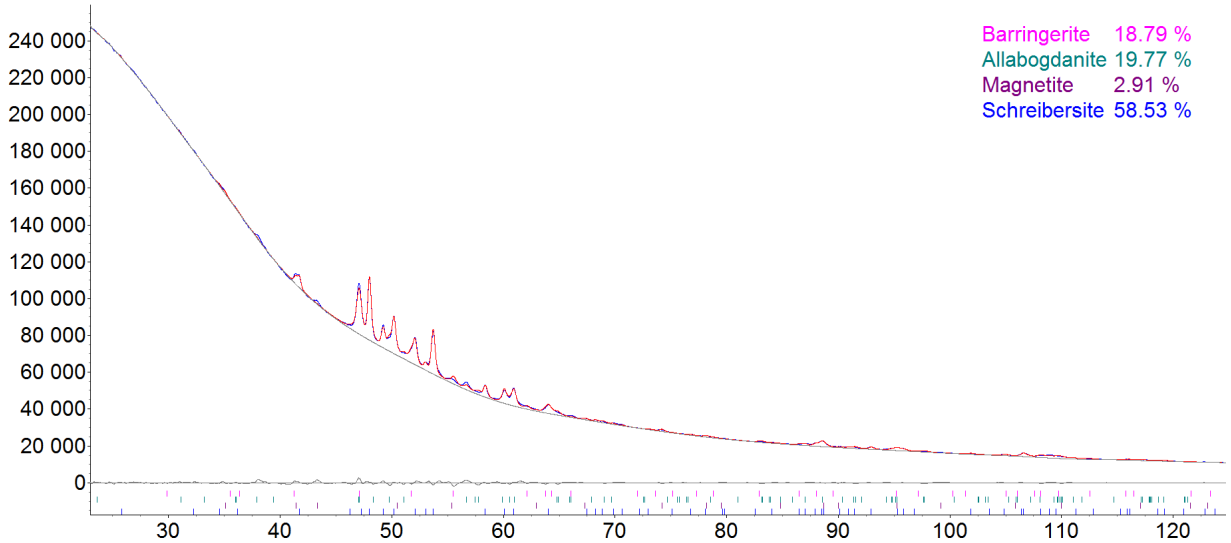

Figure S15. Rietveld refinement plot for the sample Htr (the Hatrurim Basin, Negev Desert, Israel).

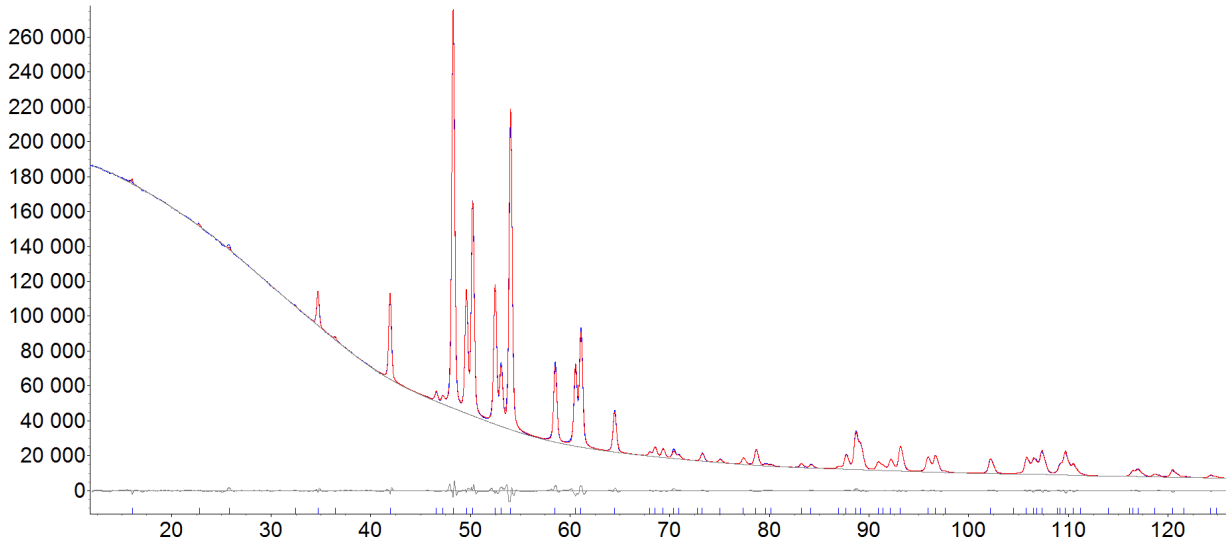

Figure S16. Rietveld refinement plot for schreibersite from the Krasnojarsk meteorite (Krs).

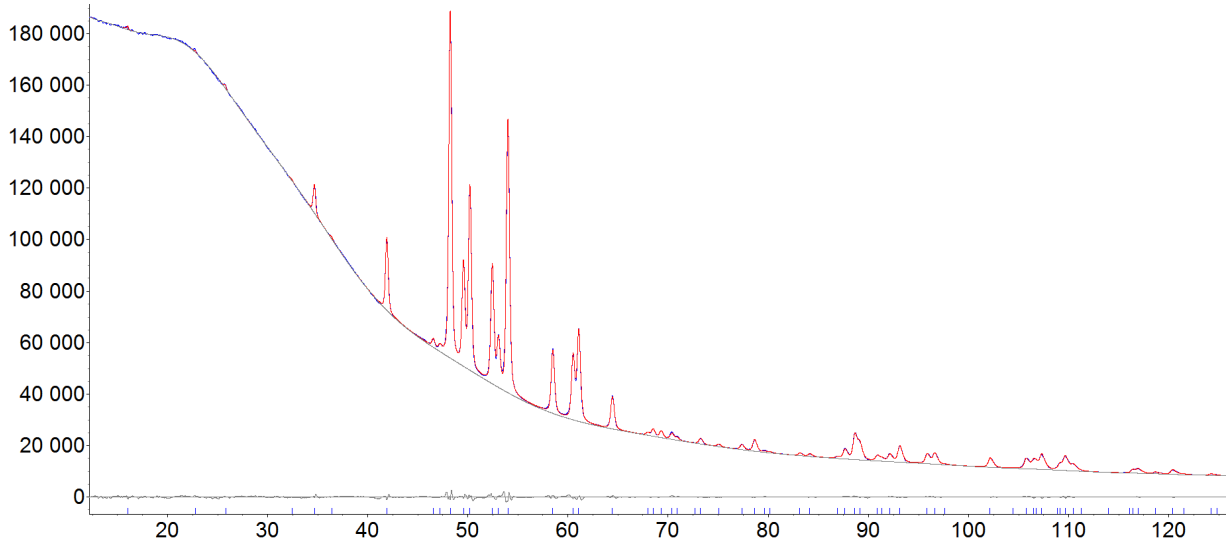

Figure S17. Rietveld refinement plot for schreibersite from the Lazarev meteorite (Lzr).

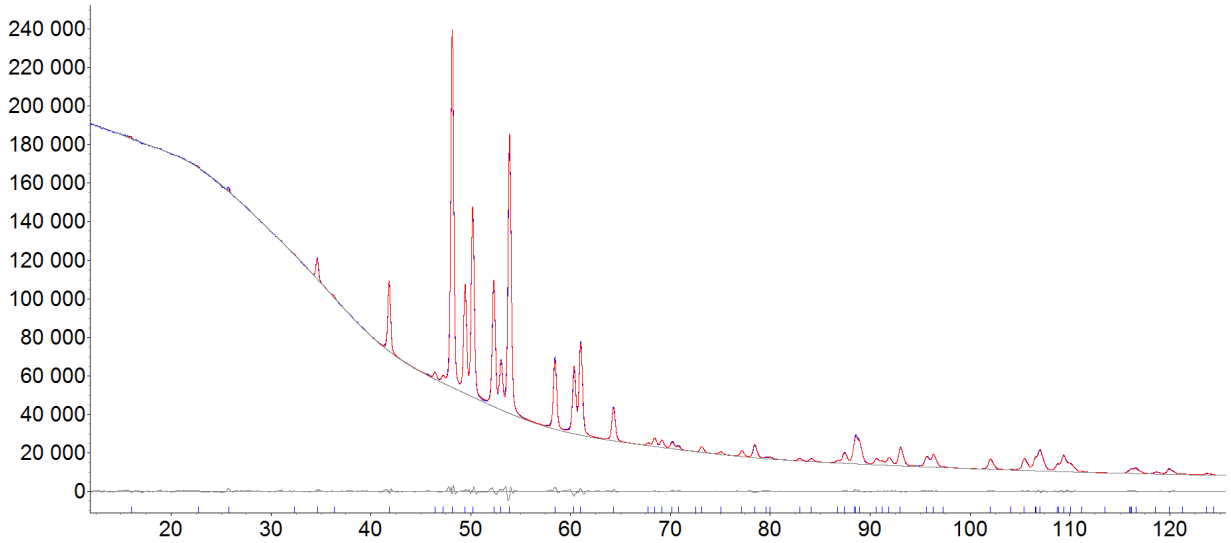

Figure S18. Rietveld refinement plot for schreibersite from the Madoc meteorite (Mad).

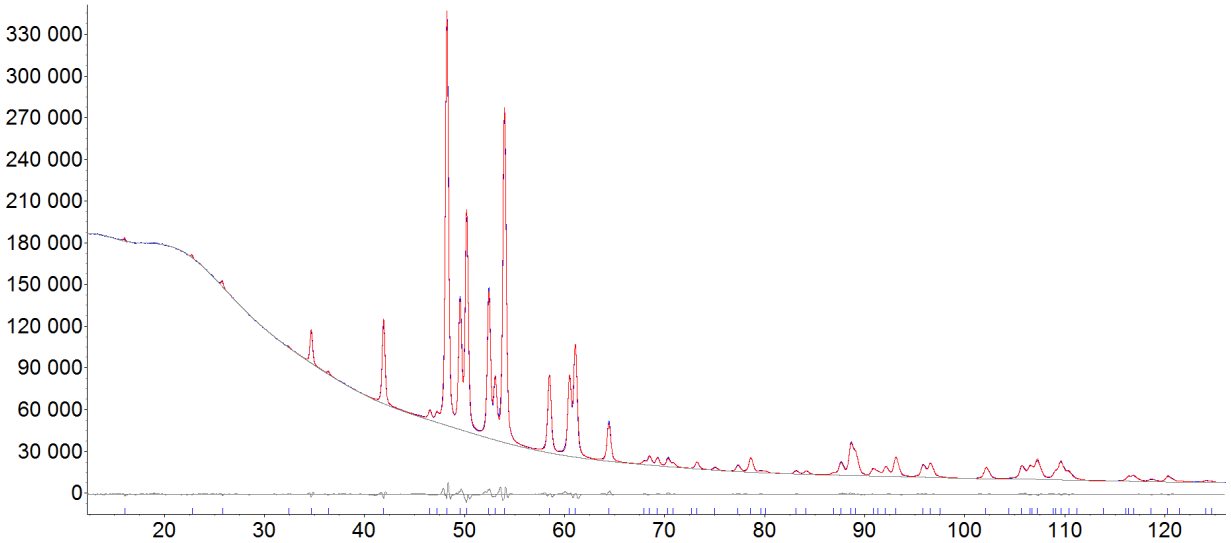

Figure S19. Rietveld refinement plot for schreibersite from the Mont Dieu meteorite (MD).

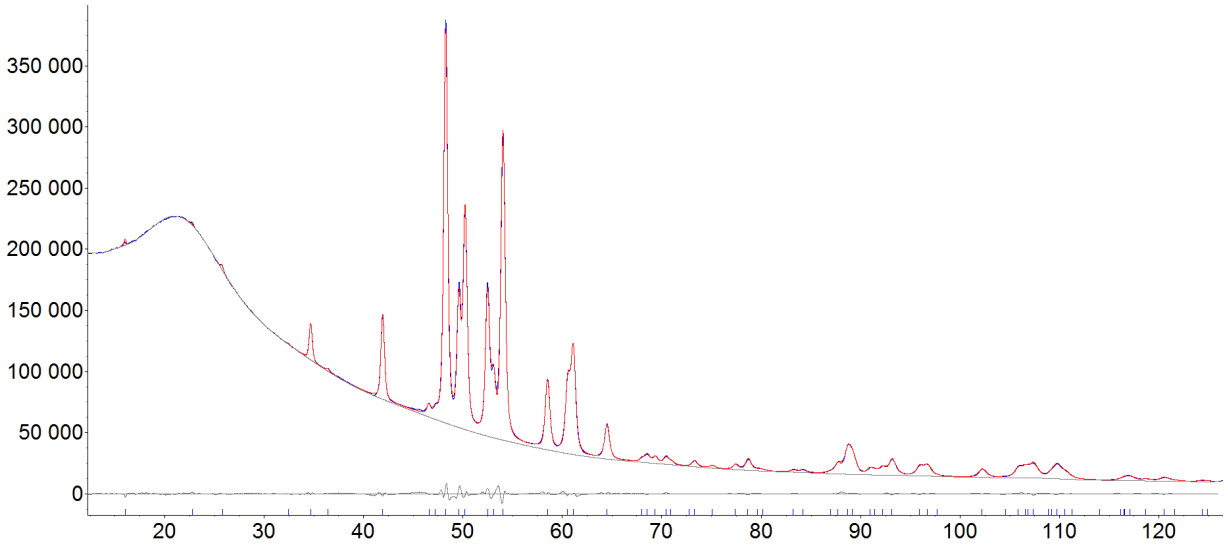

Figure S20. Rietveld refinement plot for schreibersite from the Magura meteorite (Mgr).

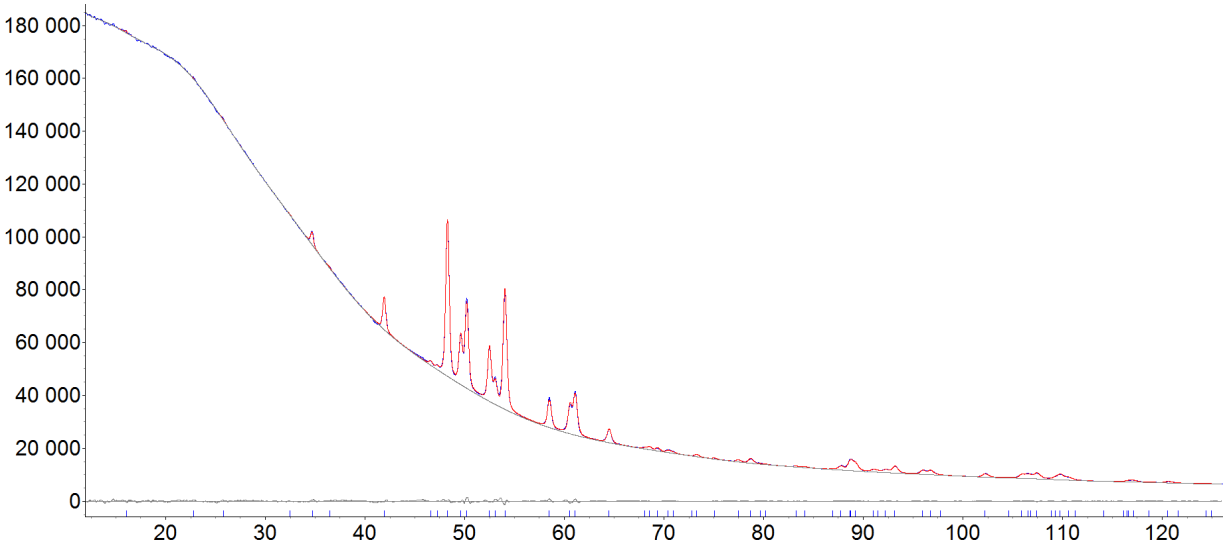

Figure S21. Rietveld refinement plot for schreibersite from the Petropavlovsk meteorite (Ptr).

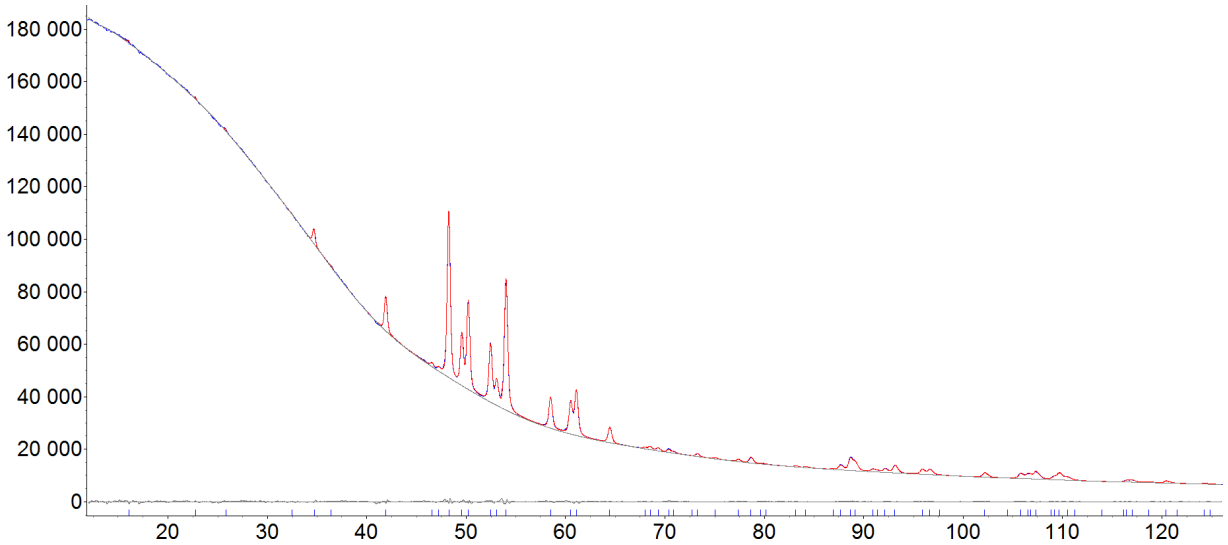

Figure S22. Rietveld refinement plot for schreibersite from the Seymchan meteorite (Sey).

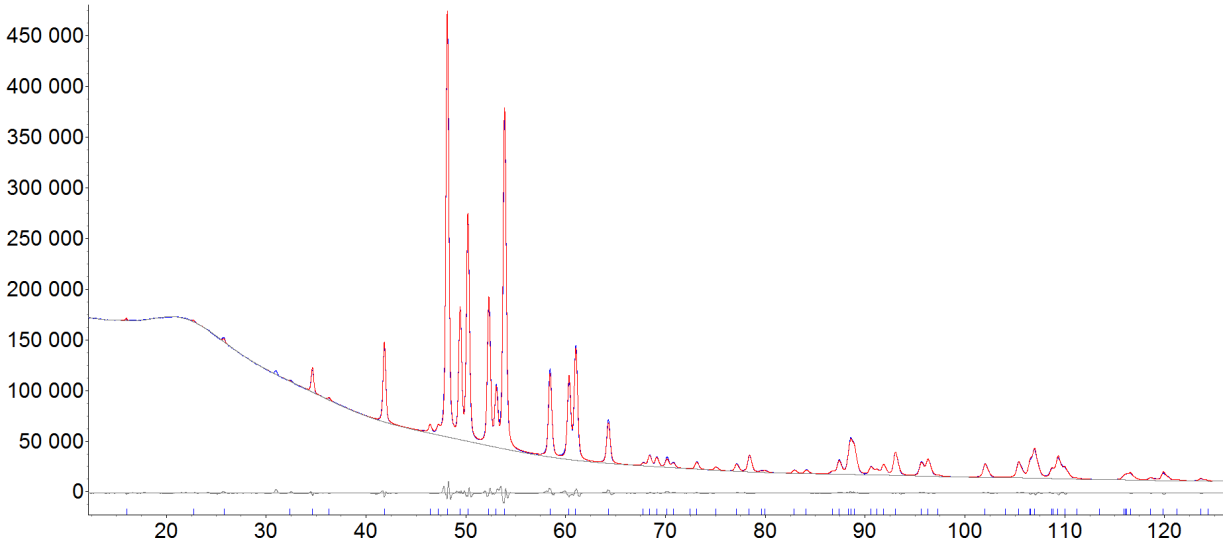

Figure S23. Rietveld refinement plot for schreibersite from the São Julião de Moreira meteorite (SJM).

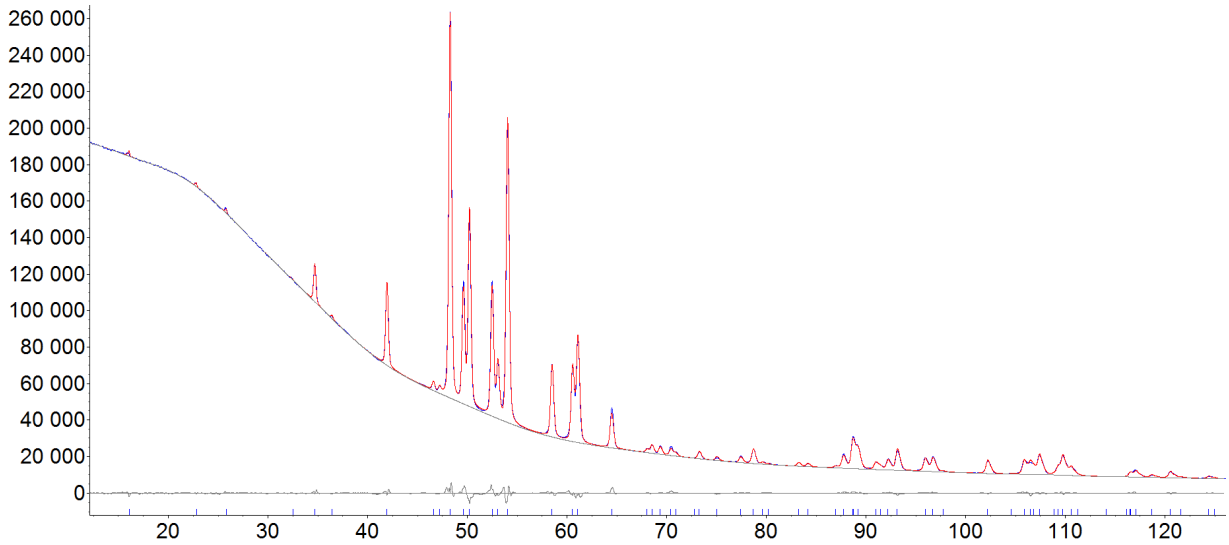

Figure S24. Rietveld refinement plot for schreibersite from the Springwater meteorite (Spr).

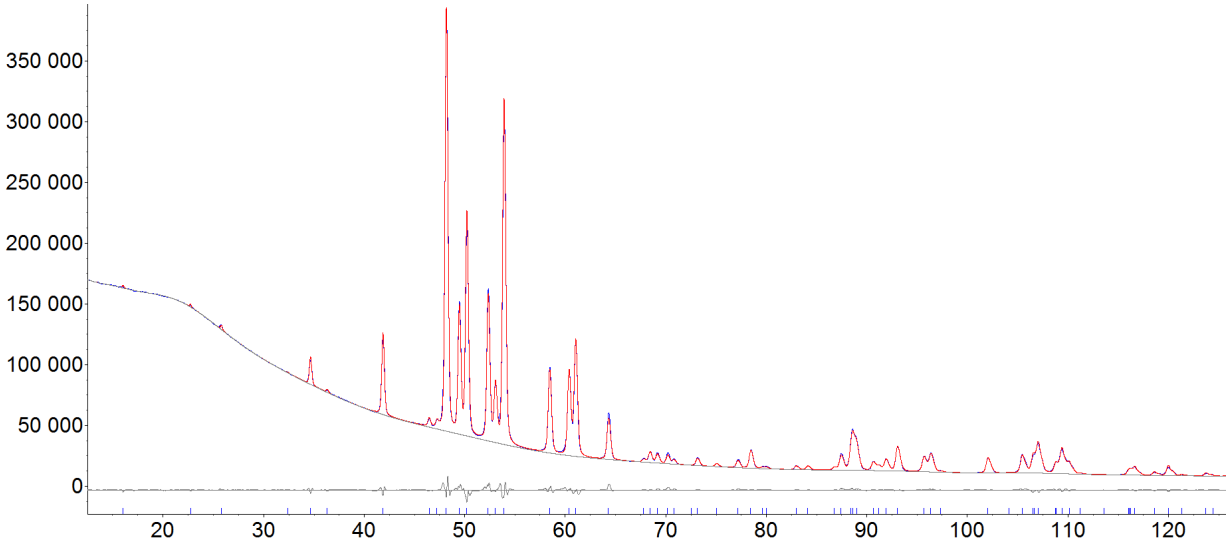

Figure S25. Rietveld refinement plot for schreibersite from the Toluca meteorite (Tol).

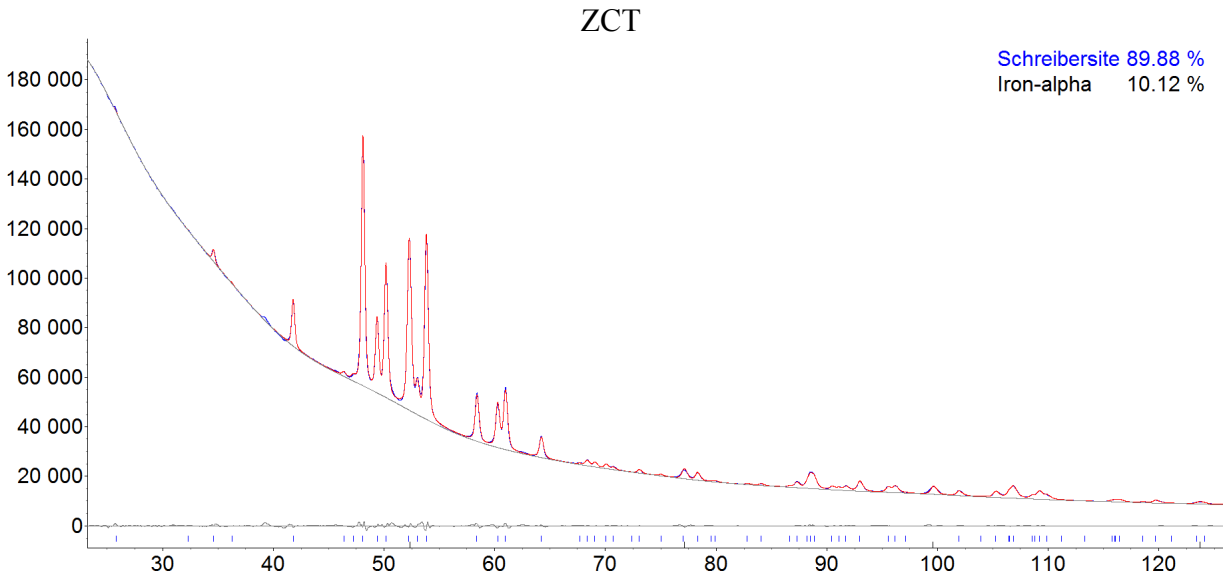

Figure S26. Rietveld refinement plot for the sample Zct [the Zacatecas (1792) meteorite].